Optical potential models used in quasielastic $^{40}Ca(e,e'p)$ calculations

Yanhe Jin and D.S. Onley
Department of Physics and Astronomy, Ohio University, Athens, Ohio 45701
(Received 24 August 1993)

Optical potentials obtained from elastic proton scattering have been successfully used to describe the final state interaction in $(e,e'p)$ reactions. However, spectroscopic factors extracted from experimental data are often quite different depending on whether relativistic calculations or nonrelativistic calculations are used. Since the calculation of the $(e,e'p)$ cross section requires the wave functions of the outgoing proton in the nuclear interior, different optical potential models could cause the differences in these calculations. We use a model which can take either nonrelativistic or relativistic optical potentials while keeping all other aspects of the calculation the same, and find that a relativistic optical potential compared with a nonrelativistic optical potential can cause a difference as much as 14%. We examined several optical models as well as the use of the Perey factor in nonrelativistic calculations.

PACS number(s): 25.30.Bf, 24.10.Ht, 27.40.+z

Exclusive $(e,e'p)$ experiments in the quasielastic region have been proven to be a good tool for studying single-particle properties of the nucleus, and have provided a testing ground for different nuclear models [1,2]. During the past few years, several high-resolution experiments have been carried out on medium/heavy nuclei at NIKHEF-K [2–6], Amsterdam. The analysis of these experimental data yields information on the single-particle wave functions and spectroscopic factors of the target nuclei. Generally, the analysis is carried out within the framework of either a relativistic distorted wave Born approximation (RDWBA) [7,8] or a nonrelativistic distorted wave Born approximation (DWBA) or Impulse approximation (DWIA) [9,10]. Both models can provide good descriptions of the data. However the extracted spectroscopic factors based on these two models are often quite different: for example, for ^{40}Ca and ^{208}Pb target nuclei, the relativistic model generally requires a spectroscopic factor which is about 10–20 % larger than the nonrelativistic model. The models require a bound-state wave function (ψ_b) and an optical potential (usually from elastic proton scattering) for the outgoing proton wave function (ψ_f), to calculate the single particle nucleon transition current

$$J^\mu = \psi_f^\dagger \hat{J}^\mu \psi_b, \tag{1}$$

where $\hat{J}^\mu$ is the free nucleon current operator. Since the various components that go into these two model calculations are from different origins, any of the components (for example, the bound-state wave function, the optical potential for the final-state interaction, the form of the current operator, the use of a Perey nonlocal factor, or the electron Coulomb distortion, etc.) could be the reason for the difference. In this paper we compare the use of different outgoing proton wave functions generated by different optical potentials which are or could be used in these calculations.

In the relativistic DWBA calculations, a global phenomenological optical potential developed by Clark and co-workers is usually used [11]. There are several new versions of these global optical potentials [12] which give equally good descriptions to the proton elastic scattering observables. This means these different potentials give essentially the same asymptotic wave functions. If the wave functions produced by these potentials are different, the differences must be in the interior part of the system. Since the $(e,e'p)$ calculation uses not only the exterior part of the wave function (phase shifts) but also the interior part of the wave function, we can use RDWBA to compare these different potentials. There are also many different nonrelativistic optical potential models one could use in the $(e,e'p)$ calculations. The one commonly used in the analysis of the experimental data is the Schwandt global optical potential [13]. We will use the Schwandt potential to compare with the relativistic optical potentials. We have also used another nonrelativistic optical potential developed by Kelly and co-workers [14], which not only can describe the elastic proton scattering but also the inelastic nucleon-nucleus scattering.

In order to see the differences caused by the different optical potentials (both relativistic and nonrelativistic) in the $(e,e'p)$ calculation, one needs to have a formalism which can take both relativistic and nonrelativistic optical potentials while keeping all the other components (like bound-state wave function, etc.) the same. One way to do this is to use the nonrelativistic formalism, then in order to use the relativistic optical potential, one needs to reduce the potential into a equivalent nonrelativistic form. However, in doing the reduction, the wave function produced by the Schrödinger calculation is often very different from the wave function produced by the Dirac calculation. In the following we describe a Dirac formalism which can take a nonrelativistic optical potential into a relativistic equation and the wave function generated (at least the large component) is the same as the corresponding nonrelativistic wave function.

We start with the Dirac equation with spherically symmetric scalar $S(r)$ and fourth-component vector $V(r)$ potentials (the SV model):

$$[\gamma_\mu p^\mu - M - S(r) - \gamma^0 V(r)]\psi = 0, \tag{2}$$

from which we can derive the radial equations

$$\frac{df}{dr} = -\frac{\kappa+1}{r} f + (E + M + S - V)g, \tag{3}$$

$$\frac{dg}{dr} = \frac{\kappa-1}{r} g + (M - E + S + V)f, \tag{4}$$

where f (g) is the upper (lower) component of the Dirac wave function and κ is the angular momentum quantum number.

We use the transformation

$$\psi' = \exp\left[\frac{1}{2}\gamma^0 \ln\left(\frac{M+E+S-V}{M+E}\right)\right]\psi \tag{5}$$

(which is one of a number of possible nonunitary transformations have been discussed extensively in Ref. [15]) after which the Dirac equation becomes

$$[\gamma^\mu p_\mu - M - \tfrac{1}{2}U(r) - \tfrac{1}{2}\gamma^0 U(r) + i\vec{\alpha}\cdot\hat{r}T(r)]\psi' = 0, \tag{6}$$

where $T(r)$ enters the equation as a tensor and $U(r)$ is a combined scalar and vector; we call this the UT model (in Ref. [17], it was called SVT model). Moreover

$$U = S + V + \frac{M - E + S + V}{M + E}(S - V), \tag{7}$$

$$T = -\frac{1}{2}\frac{d}{dr}\ln(M + E + S - V). \tag{8}$$

The radial equations become

$$\frac{dF}{dr} = \left(-\frac{\kappa+1}{r} + T(r)\right)F + (E + M)G, \tag{9}$$

$$\frac{dG}{dr} = \left(\frac{\kappa-1}{r} - T(r)\right)G + (M - E + U)F, \tag{10}$$

where the new radial functions $F(r)$ and $G(r)$ are related to those from the SV model as

$$f = C_{\rm rel}F, \qquad g = C_{\rm rel}^{-1}G, \tag{11}$$

where

$$C_{\rm rel} = \sqrt{\frac{M + E + S - V}{M + E}}. \tag{12}$$

In nuclei $S - V$ is negative and the factor $C_{\rm rel}$ has the effect of reducing the large component f compared to F inside the nucleus and enhance the lower component g by the same amount (fg and FG are the same); outside S and V are zero and f and F will have the same asymptotic properties.

The advantage of the UT form is that the large component F obeys Schrödinger-like equations. In particular, eliminating the lower component:

$$\frac{d^2F}{dr^2} + \frac{2}{r}\frac{dF}{dr} - \frac{\kappa(\kappa+1)}{r^2}F$$

$$-2M\left[V_{\rm cen} + V_{\rm so}(-\kappa - 1)\right]F + p^2F = 0. \tag{13}$$

We recognize $\kappa(\kappa+1)$ and $(-\kappa-1)$ as the eigenvalues of L^2 and $\sigma\cdot L$, respectively, so we have a Schrödinger equation with energy-dependent central and spin-orbit potentials:

$$V_{\rm cen} = \frac{M+E}{2M}U + \frac{1}{2M}\left(\frac{dT}{dr} + T^2 + \frac{2T}{r}\right), \tag{14}$$

$$V_{\rm so} = \frac{T}{Mr}. \tag{15}$$

From the foregoing we note the following: First, since there is no approximation involved, one may obtain F either from the UT equations (9) and (10) or the Schrödinger equation (13). The solutions can differ only by an overall normalization constant. For example, in Fig. 1 we show the $d_{5/2}$ bound-state wave functions (F and G) from solving Eqs. (9) and (10) as dashed lines, and from solving Eq. (13), as a dotted curve. This shows that the contribution from the lower component of the UT wave function is unimportant, that the normalization is essentially the same as the nonrelativistic calculation and emphasizes the equivalence of the Schrödinger model and UT model. The SV solutions [Eqs. (3) and (4)] are also shown for comparison. Second, although

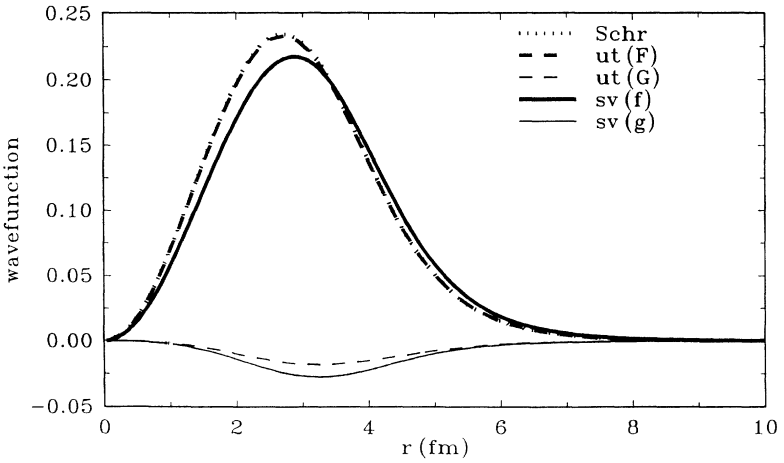

FIG. 1. The $d_{5/2}$ bound-state wave function F obtained from solving either the Dirac UT equation (upper and lower components, dashed lines) or the Schrödinger equation (dotted line). For comparison, we also show the wave function (upper and lower components, solid lines) from solving the Dirac SV model.

the Schrödinger wave functions can be made equivalent to Dirac UT solutions, to be compared with the more common SV wave functions one must use the factor $C_{\rm rel}$ from Eq. (12); in its effect, this is comparable with the Perey factor which is commonly included in nonrelativistic calculations. Third, the residual small component G is related by Eqs. (9) and (10) to the large component F

$$G = \frac{1}{E+M}\left[\frac{dF}{dr} + (\frac{\kappa+1}{r} - T)F\right] \tag{16}$$

which, aside from the factor T which is commonly small for nuclear potentials, is the same relation as for a free particle. Thus it is a defensible procedure to enhance a nonrelativistic wave function by introducing a lower component using the Dirac free-particle relation, as is sometimes done to get an equivalent relativistic wave function [16]. Fourth, the lower component G is affected only by potentials which vanish in the nonrelativistic limit and which, in the case of nuclear potentials, are very weak. Thus negative-energy solutions, since G now is the large component, will be little affected and vacuum polarization is minimal. In this respect the model is very different from the SV potentials where the effective central potential for negative-energy states not only survives in the nonrelativistic limit but also is much stronger than that for the positive-energy states [17].

We will use these connections to compare the use of different proton optical potentials (some nonrelativistic and some relativistic) in the $(e, e'p)$ reaction. For the Dirac SV calculation we take the final-state proton wave function $\psi_f = \psi$ from Eq. (1). For the UT relativistic calculation $\psi_f = \psi'$ from Eq. (6). For the nonrelativistic potentials, U and T are obtained from Eqs. (14) and (15) and Eq. (6) is again used. This way of comparing different optical models has one particular advantage, all other aspects of the calculation (the bound-state wave function, the current operator, etc.) can remain unchanged, thus it can separate the relativistic effect from the effects due to the use of different potentials. Comparison of the SV model with the corresponding UT model will show the relativistic effect; comparison of different central + spin-orbit type potentials (whether relativistic or nonrelativistic) can be done using the UT model.

Before we discuss the specific effects on $(e, e'p)$ we make some general observations. Equivalent potentials are generally deemed unsatisfactory if a smooth potential generates an oddly shaped equivalent which could certainly happen here. In a sense what is mathematically equivalent may be physically implausible. But smooth S, V potentials of the Wood-Saxon (WS) shape lead to smooth U, T potentials and ultimately to smooth $V_{\rm cen}$, $V_{\rm so}$ potentials. For example, the $V_{\rm so}$ potential shape is related to the derivative of the WS shape, i.e., is surface peaked but not given precisely by the Thomas relation. A Coulomb potential in the original SV equation gives an equation which is asymptotically Coulomb plus Thomas spin-orbit coupling but there are other long-ranged contributions from the same term which means that the phase-shift equivalency does not extend to Coulomb phases.

The results we will present below were calculated using the same relativistic bound-state wave functions (derived from a Hartree calculation—the σ-ω model). Since we just want to look at the effect of using different relativistic and nonrelativistic optical potentials for the knocked-out proton, the electron is treated in the plane wave Born approximation. The electron incident energy is 500 MeV and the kinetic energy for knocked-out proton is 135 MeV. All the results were calculated using parallel kinematics, i.e., the proton is ejected in the same direction as the momentum transfer to the nucleus. These conditions are chosen because they correspond to known experimental results from NIKHEF. One usually presents the experimental data in the form of a reduced cross section [1]:

$$\rho(p_m) = \frac{1}{pE\sigma_{ep}^{cc1}} \frac{d^3\sigma}{d\Omega_e d\Omega_p dk_0'}, \tag{17}$$

where (σ_{ep}^{cc1}) is the off-shell electron-proton cross section defined in Ref. [18] and p_m is the missing momentum defined by $p_m = p - q$. In the plane-wave impulse approximation (PWIA), when all the electron and proton distortions are neglected, the quantity ρ is the momentum density of the bound proton.

In Fig. 2 we show the results of knocking out a proton from (a) the $d_{3/2}$ state and (b) the $2s_{1/2}$ state of ^{40}Ca using different relativistic optical potentials. The solid line

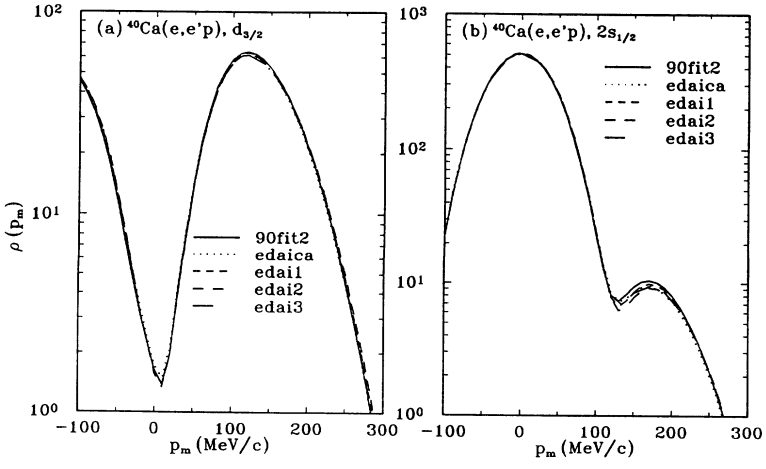

FIG. 2. Calculation of knocking out a proton from (a) $d_{3/2}$ state and (b) $2s_{1/2}$ state of ^{40}Ca using different relativistic optical potentials.

(90fit2) represents the results of using the 1990 global optical potential (fit2) [11]. The dotted line (edaica) represents a potential which has been fitted only to the ^{40}Ca data [12]: the results are evidently very close. All the other curves (edai1, edai2, edai3) are from the use of the 1993 global optical potentials [12]. The difference between all these curves is no more than 2% which is much smaller than any corresponding experimental error. So we can conclude that the different versions of the relativistic optical potential cannot be distinguished by the $(e, e'p)$ reaction. However, we need to make two points here: (1) all these different versions of the relativistic optical potentials are forms of the relativistic Scalar-Vector (SV) model; if a non-SV dominant model (like UT model) is used, the difference can be larger; (2) the conclusion is based on calculations at one proton kinetic energy (135 MeV), one needs to look at over a much broader range in order to generalize the conclusion. In later comparisons to the nonrelativistic models we will only show one relativistic curve (90fit2).

In Fig. 3 we show the results of knocking out a proton from the $d_{3/2}$ state of ^{40}Ca using both relativistic and nonrelativistic optical potentials. The thick solid line represents relativistic optical potentials. The thin dashed line (kelly) represents the nonrelativistic Kelly potential [14] and the thin dotted line (schwa) represents the Schwandt potential [13]. We can see that the Schwandt potential gives a strength which is more than 14% larger than the relativistic potential around the peak. The Kelly potential (which is obtained by fitting to the inelastic nucleon-nucleus scattering) gives a strength about 6% larger. We show the corresponding UT calculation, derived using Eqs. (7) and (8) from the SV potentials, as the thin solid line (ut). The difference between the UT (ut) and SV (90fit2) calculations is caused by the relativistic factor $C_{\rm rel}$. One can immediately see that the agreement between the calculations from the Kelly potential and the relativistic UT potential is very good, which tells us that the main difference between the Kelly potential and the Dirac (SV) potential is just a relativistic effect. The calculation from the Schwandt potential does not agree well with the UT calculation. Basically the calculation from the Schwandt potential gives the wrong shape. In other words, if one applied the relativistic factor $C_{\rm rel}$ to the nonrelativistic calculations, one would have nonrelativistic calculations comparable to the relativistic (SV) results.

In nonrelativistic calculations, it is common to reduce the interior wave function by a Perey factor. The factor used in the analysis of the experimental data performed at NIKHEF [6] has the form

$$C_p = 1/\sqrt{1 - V\left(\frac{\mu\beta^2}{2\hbar^2}\right)}, \tag{18}$$

where V is a local optical potential, μ is the reduced mass, and β a nonlocality range parameter determined some time ago by Perey [19]. The value commonly used is $\frac{\mu\beta^2}{2\hbar^2} = 1/115$ MeV^{-1}. Including this factor in the Schwandt and Kelly potentials, we get the results shown in thick dotted and dashed lines in Fig. 3. It is remarkable that the effect of the Perey factor on the Kelly potential (compare thin and thick dashed lines) is very much the same as the effect of $C_{\rm rel}$ in the relativistic potentials (compare thin and thick continuous lines). We would like to address the question of whether these factors are equivalent.

The Perey factor was introduced to allow for the nonlocality associated with the nuclear potential. The dominant contribution is from the central potential $V_{\rm cen}$, which corresponds roughly in the SV model to $S + V$. The relativistic factor $C_{\rm rel}$, using Eqs. (8), (12), and (15), can be related to the combination $S - V$ or to the nonrelativistic spin-orbit potential; explicitly

$$C_{\rm rel} = \exp\left\{\int_r^\infty M r V_{\rm so} dr\right\}. \tag{19}$$

Thus these two factors are not the same and can be ascribed to different physical origins; nor are they really, in closer examination, of comparable size. In Fig. 4 we show the real parts of these two factors (the imaginary parts

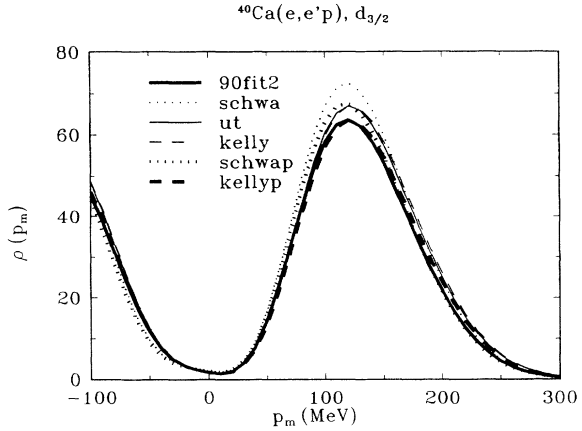

FIG. 3. Calculation of knocking out a proton from $d_{3/2}$ state using both relativistic and nonrelativistic optical potential. Note this is shown on a linear scale for clarity.

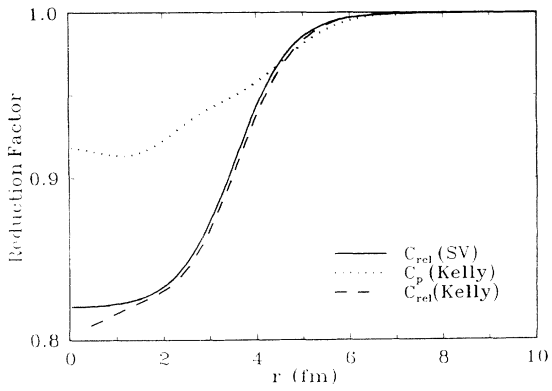

FIG. 4. The real part of the Perey factor (dotted line) calculated using the Kelly potential and the real part of the relativistic factor calculated using either the SV potential (solid line) or the Kelly potential (dashed line).

are 2 orders smaller) calculated using Eqs. (18) and (19) and the Kelly potential. It is also interesting to note that the $C_{\rm rel}$ (solid line), calculated using the SV potential, agrees quite well with the one from the Kelly potential. This leaves open the question of whether one should include both factors in nonrelativistic calculations. To justify this one would have to show that one could include a nonlocal effect in relativistic calculations in a fashion similar to that of Perey (this is under investigation).

In Fig. 5 we show the same calculations as in Fig. 3 but knocking out a proton from $2s_{1/2}$ state. We can see that in this case, differences around the first peak from using different optical potentials are very small. Most of the differences show around the second peak. That is because the $2s_{1/2}$ state is distributed differently from the $d_{3/2}$ state in r space. Also here again the results from the Kelly potential agree quite well with the UT calculation while the results from the Schwandt potential do not agree well.

In conclusion, we described a model which can enable us to compare the nonrelativistic optical potentials with the relativistic potentials in the $(e, e'p)$ calculation while keeping all the formalism relativistic. Different versions of the relativistic global optical potential developed by Clark and co-workers make a difference less than 2% in the $(e, e'p)$ calculations. The Kelly potential gives about the same result as the relativistic UT potential. The Schwandt potential gives the same magnitude as the UT potential but the shape is different. If we compare the nonrelativistic calculations to the relativistic calculations (SV) directly, for $d_{3/2}$ state, using the Schwandt potential can cause an enhancement as much as 14% around the peak while the Kelly potential can cause 6%, which is caused mainly by the relativistic effect. The Perey factor used in the nonrelativistic DWIA calculation plays a less significant role than the relativistic factor $C_{\rm rel}$. Since the relativistic factor can explain partially why the spectroscopic factors extracted based on the nonrelativistic calculations are lower, we suggest, for comparison purposes, the relativistic factor should be included in the optical model wave functions.

The transformations we describe above can also be applied to bound-state wave functions; one might question whether it is consistent to change the final proton state in this way without making the corresponding transformation in the initial state. To understand this one must remember that the constraints imposed on the two states are rather different. For the free states we need to reproduce the proton scattering results which means we are constrained to reproduce the right set of phase shifts; we do this by adopting a transformation which leaves the

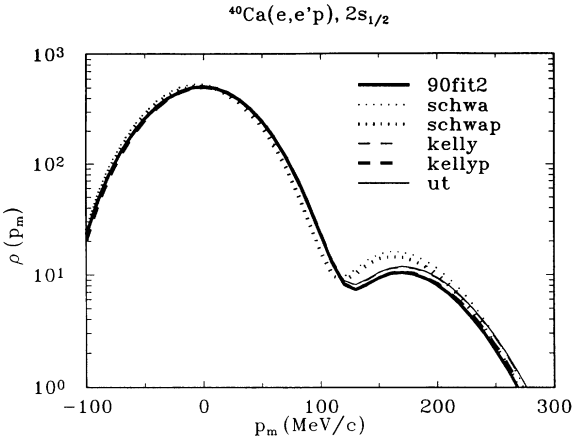

FIG. 5. Same as Fig. 3 but knocking out a proton from $2s_{1/2}$ state. In this case a logarithmic scale is used to show differences at lower peek.

asymptotic form of the wave function unchanged. The same transformation, applied to a bound state evidently leaves the binding energy unchanged. This may seem desirable but it is not essential. The initial proton wave function is actually an effective single particle wave function formed by the overlap $\langle {}^{A-1}_{N}X_{Z-1}|{}^{A}_{N}X_{Z}\rangle$ between the entire initial and final nuclear wave functions and is not necessarily a solution of a single particle equation at all. On the other hand making the transformation from SV to UT form changes the radius of the particle distribution seriously, and hence would violate the more sensitive criterion that we reproduce the right nuclear radius (our Hartree and Hartree-Fock wave functions do this). We could use corresponding nonrelativistic Hartree -Fock calculations but this would introduce a whole new range of options, and in any case, are not used in the experimental analysis: there the effective single-particle wave function is treated as an unknown and adjusted to fit the data. Thus the question of the appropriate treatment of the initial proton wave function is complex and reduces to the question of what one considers to be the right set of nuclear observables to match. Ultimately one should compare all assumptions which go into a wholly nonrelativistic calculation with those used in the relativistic calculations (currently being undertaken [20]).

We would like to thank H.P. Blok for helpful discussions. Collaboration with NIKHEF was supported in part by NATO Collaborative Research Grants Programme CRG 921258. This work was supported in part by the U.S. Department of Energy under Grant No. DE-FG02-87ER40370.

[1] S. Frullani and J. Mougey, Adv. Nucl. Phys. **14**, 1 (1984).
[2] L. Lapikás, Nucl. Phys. **A553**, 297c (1993).
[3] G. van der Steenhoven, H.P. Blok, E. Jans, L. Lapikás, E.N.M. Quint, and P.K.A. de Witt Huberts, Nucl. Phys. **A484**, 445 (1988).
[4] J.W.A. den Herder, H.P. Blok, E. Jans, P.H.M. Keizer, L. Lapikás, E.M.N. Quint, G. van der Steenhoven, and P.K.A de Witt Huberts, Nucl. Phys. **A490**, 507 (1988).
[5] E.M.N. Quint, Ph.D. dissertation, University of Amsterdam, 1988.

[6] G.J. Kramer, Ph.D. dissertation, University of Amsterdam, 1990.
[7] Yanhe Jin, D.S. Onley, and L.E. Wright, Phys. Rev. C **45**, 1311 (1992).
[8] Yanhe Jin, J.K. Zhang, D.S. Onley, and L.E. Wright, Phys. Rev. C **47**, 2024 (1993).
[9] C. Giusti and F. Pacati, Nucl. Phys. **A473**, 717 (1987).
[10] C. Giusti and F. Pacati, Nucl. Phys. **A485**, 461 (1988).
[11] S, Hama, B.C. Clark, E.D. Cooper, H.S. Sherif, and R.L. Mercer, Phys. Rev. C **41**, 2737 (1990).
[12] S. Hama, B.C. Clark, E.D. Cooper, H.S. Sherif, and R.L. Mercer, Phys. Rev. C **47**, 297 (1993).
[13] P. Schwandt, H.O. Meyer, W.W. Jacobs, A.D. Bacher, S.E. Vigdor, M.D. Kaichuck, and T.R. Donoghue, Phys. Rev. C **26**, 55 (1982).
[14] J.J. Kelly, Phys. Rev. C **39**, 2120 (1989); and private communication.
[15] B.C. Clark, S. Hama, S.G. Kälbermann, E.D. Cooper, and R.L. Mercer, Phys. Rev. C **31**, 694 (1985).
[16] Yanhe Jin, L.E. Wright, C. Bennhold, and D.S. Onley, Phys. Rev. C **38**, 923 (1988).
[17] Yanhe Jin and D.S. Onley, Phys. Rev. C **38**, 813 (1988).
[18] T. DeForest, Jr., Nucl. Phys. **A392**, 232 (1983).
[19] F.G. Perey and B. Buck, Nucl. Phys. 32, 353 (1962).
[20] H.P. Blok, private communication.